Article

Cell Reports

Forward Genetic Screens in Zebrafish Identify Pre-mRNA-Processing Pathways Regulating Early T Cell Development

Graphical Abstract

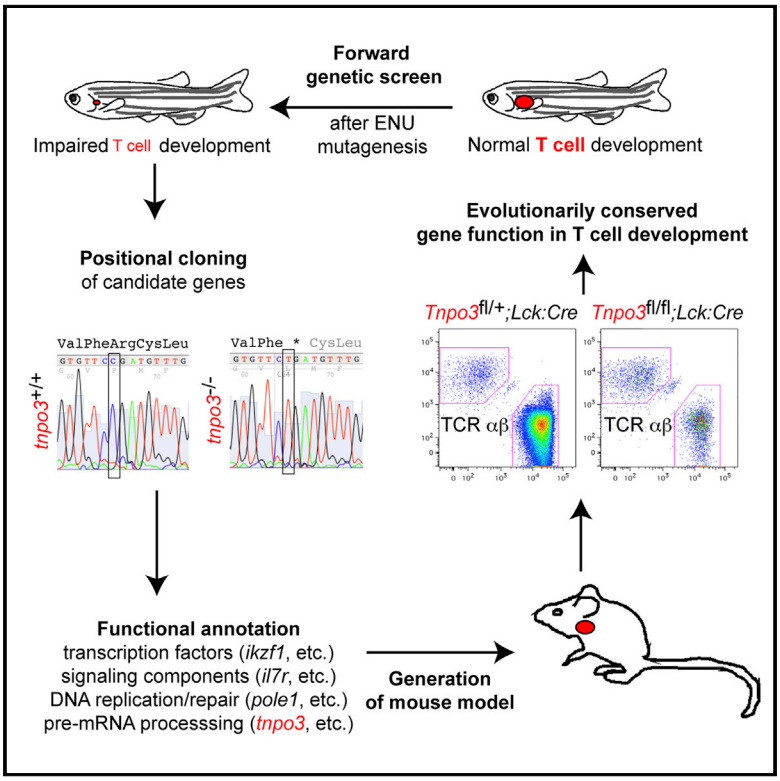

Authors

Norimasa Iwanami, Katarzyna Sikora, Andreas S. Richter, ..., Connor P. O'Meara, Michael Schorpp, Thomas Boehm

Correspondence

boehm@immunbio.mpg.de

In Brief

Using forward genetic screens in zebrafish, Iwanami et al. identify evolutionarily conserved functions in T cell development of transcription factors (such as *ikzf1*), signaling components (such as *il7r*), DNA replication/repair genes (such as *pole1*), and certain pre-mRNA-processing factor genes (such as *tnpo3*).

Highlights

- Forward genetic screens identify mutations affecting zebrafish T cell development
- Identification of *il7r*, *jak3*, and *pole1* mutations validates specificity of screen design
- Mutations in pre-mRNA-processing factor genes reveal evolutionarily conserved pathway
- In zebrafish and mice, TNPO3 deficiency impairs T cell differentiation

Accession Numbers

GSE77480

Iwanami et al., 2016, Cell Reports *17*, 2259–2270
November 22, 2016
http://dx.doi.org/10.1016/j.celrep.2016.11.003

Cell Reports
Article

OPEN ACCESS
CellPress

Forward Genetic Screens in Zebrafish Identify Pre-mRNA-Processing Pathways Regulating Early T Cell Development

Norimasa Iwanami,[1] Katarzyna Sikora,[1,2] Andreas S. Richter,[2,3] Maren Mönnich,[1,4] Lucia Guerri,[1,5] Cristian Soza-Ried,[1,6] Divine-Fondzenyuy Lawir,[1] Fernando Mateos,[1] Isabell Hess,[1] Connor P. O'Meara,[1] Michael Schorpp,[1] and Thomas Boehm[1,7,*]

[1]Department of Developmental Immunology
[2]Bioinformatics Unit
Max Planck Institute of Immunobiology and Epigenetics, Stuebeweg 51, 79108 Freiburg, Germany
[3]Present address: Genedata AG, 4053 Basel, Switzerland
[4]Present address: Wilhelm Johannsen Centre for Functional Genome Research, Department of Cellular and Molecular Medicine, University of Copenhagen, Blegdamsvej 3, 2200 Copenhagen, Denmark
[5]Present address: Laboratory of Neurogenetics, NIAAA, NIH, 5625 Fishers Lane, Rockville, MD 20852-1728, USA
[6]Present address: Fundación Oncoloop, Antonio Varas 710, Santiago and Universidad Andrés Bello, Facultad de Medicina, República 330, Santiago, Chile
[7]Lead Contact
*Correspondence: boehm@immunbio.mpg.de
http://dx.doi.org/10.1016/j.celrep.2016.11.003

SUMMARY

Lymphocytes represent basic components of vertebrate adaptive immune systems, suggesting the utility of non-mammalian models to define the molecular basis of their development and differentiation. Our forward genetic screens in zebrafish for recessive mutations affecting early T cell development revealed several major genetic pathways. The identification of lineage-specific transcription factors and specific components of cytokine signaling and DNA replication and/or repair pathways known from studies of immunocompromised mammals provided an evolutionary cross-validation of the screen design. Unexpectedly, however, genes encoding proteins required for pre-mRNA processing were enriched in the collection of mutants identified here. In both zebrafish and mice, deficiency of the splice regulator TNPO3 impairs intrathymic T cell differentiation, illustrating the evolutionarily conserved and cell-type-specific functions of certain pre-mRNA-processing factors for T cell development.

INTRODUCTION

All vertebrates share the same basic principle of lymphocyte differentiation along distinct T-cell-like and B-cell-like lineages (Boehm, 2011; Hirano et al., 2013), suggesting that the genetic program regulating the developmental pathways of lymphocytes must have already existed in a common ancestor for all vertebrates. Taking advantage of the apparent evolutionary conservation of lymphocyte-based immunity, we conducted genetic screens in zebrafish aimed at identifying previously unknown regulators of T lymphocyte development. Zebrafish is particularly suited for such an analysis, as T cell development already begins in the embryo during the third day after fertilization (Langenau and Zon, 2005). During these early stages of embryonic development, maternal factors are expected to buffer, at least partially, the phenotypic consequences of zygotic defects in mutant fish unless particular cell types (T cells in the present case) exhibit a specific requirement for the unimpaired activity of a certain gene(s). We therefore expected that this unique biological feature of T cell development in zebrafish would allow us to identify cell-type-specific functions of genes that are also required for stages of development prior to the onset of lymphopoiesis. A similar approach would not be feasible in mammals, because their lymphocytes develop at a considerably later point in embryogenesis; as a consequence, in mice, for instance, embryonic lethality often masks subsequent lineage-specific functions of pleiotropically acting genes, for example *Gata3* (Pandolfi et al., 1995).

In the mouse, specific networks of transcription factors have been shown to regulate the three major phases of T cell development. In the initial phase, T cell progenitors are generated and recruited to the thymus; subsequently, they are induced to adopt a T cell fate; finally, they become responsive to signals emanating from the T cell receptor (Yui and Rothenberg, 2014). Hence, assuming that these regulatory circuits emerged at an early stage in vertebrate evolution, a comprehensive genetic screen of T cell development in zebrafish would be predicted to identify at least some of the factors governing these three phases. In keeping with this expectation, we identified mutations in genes encoding lymphoid lineage-specific transcription factors, and components of cytokine signaling and DNA replication/repair pathways. Quite unexpectedly, however, pre-mRNA-processing factors were also found to play a specific role in T cell development. Using genetic interaction analysis and transcriptome profiling, we established a functional network of certain

Table 1. Identification of 15 Genes Associated with Impaired T Cell Development in Zebrafish Larvae

Mutant[a]	Allele[a]	Affected Gene[b]		Molecular Defect[c]	Reference
Hematopoietic Development					
IP109	t25127	*cmyb*	(ENSDARG00000053666)	p.I181N mis-sense mutation	Soza-Ried et al., 2010
IT325	t24980	*ikzf1*	(ENSDARG00000013539)	p.Q361X non-sense mutation	Schorpp et al., 2006
II032	t25880	*ikzf1*	(ENSDARG00000013539)	p.R489X non-sense mutation	this paper[d]
HY022	t21380	*il7r*	(ENSDARG00000078970)	p.L124FfsX5 frameshift mutation	Iwanami et al., 2011
HX157	t22598	*jak1*	(ENSDARG00000020625)	p.R580X non-sense mutation	Iwanami et al., 2011
IP045	t25078	*jak3*	(ENSDARG00000010252)	p.Q336X non-sense mutation	Iwanami et al., 2011
DNA Replication/Repair					
HI064	t22406	*top3a*	(ENSDARG00000052827)	p.E331X non-sense mutation	Mönnich et al., 2010
WW20/12	fr17	*top3a*	(ENSDARG00000052827)	p.I531S mis-sense mutation	Mönnich et al., 2010
HG010	t20320	*pole1*	(ENSDARG00000058533)	p.I633K mis-sense mutation	this paper[d]
IG335	t23336	*mcm10*	(ENSDARG00000045815)	p.L248R mis-sense mutation	this paper[d]
IY071	t25501	*dnmt1*	(ENSDARG00000030756)	p.N1391K mis-sense mutation	this paper[d]
HK017	t20463	*zbtb17*	(ENSDARG00000074548)	p.Q562K mis-sense mutation	this paper[d]
Pre-mRNA Processing					
KW059	t26426	*snapc3*	(ENSDARG00000071237)	p.C297X non-sense mutation	this paper
WW18/10	fr100	*lsm8*	(ENSDARG00000091656)	p.E72X non-sense mutation	this paper
KL069	t26393	*gemin5*	(ENSDARG00000079257)	p.Y437X non-sense mutation	this paper
HA343	t22074	*tnpo3*	(ENSDARG00000045680)	p.R203X non-sense mutation	this paper[d]
IU191	t25877	*cstf3*	(ENSDARG00000018904)	p.D313VfsX7 frameshift mutation[e]	this paper[d]

[a]WW20/12 and WW18/10 lines originate from the Freiburg (allele designation **fr**x) gynogenetic screen; all other lines (allele designation **t**x) originate from the Tübingen 2000 screen.
[b]Genes (ENSEMBL identifiers) marked in red have previously been associated with human immunodeficiency syndromes: *IL7R* (Puel et al., 1998); *JAK3* (Russell et al., 1995); *POLE1* (Pachlopnik Schmid et al., 2012); *ikzf1* is also known as *ikaros*.
[c]Molecular defects designated according to nomenclature in den Dunnen and Antonarakis (2000).
[d]Full details for these mutations will be reported elsewhere.
[e]As a result of a splice mutation (Zv9; g.18:44,161,594G > A).

components of the pre-mRNA splicing machinery and demonstrated that the role of this network for T cell development is evolutionarily conserved.

RESULTS

Outcome of Forward Genetic Screens in Zebrafish

Two genetic screens were conducted in zebrafish to identify recessive mutations affecting T lymphocyte development (Boehm et al., 2003; Schorpp et al., 2006). To this end, the expression of *rag1* was determined at 5 days post-fertilization (dpf) by RNA in situ hybridization. The product of the *rag1* gene is essential for T cell receptor assembly in developing T cells in the thymus, the first site of lymphopoiesis in zebrafish embryos. Only mutant fish with no overt developmental abnormalities apart from impaired intrathymic T cell development were considered for further characterization. Together with the Tübingen 2000 screen consortium, we screened F_3 clutches of 4,584 F_2 families, representing 4,253 mutagenized haploid genomes; so far, 42 lines carrying recessive mutations affecting *rag1* expression levels could be established. The Freiburg gynogenetic screen of 281 genomes led to the establishment of three lines, all of which were found to harbor recessive mutations. Owing to the considerable efforts associated with isolating mutated genes by positional cloning, we conducted an interim analysis after the identification of more than one-third of affected genes. The results of this analysis are reported here.

The pertinent features of the first 15 complementation groups, for which the affected genes were identified by linkage analysis and positional cloning (in two cases, aided by whole-genome sequencing), are summarized in Table 1. The fact that, among the first 17 of the 45 mutant lines analyzed here, two genes (*ikzf1* and *top3a*) were represented by two distinct alleles each suggests that our screen was near saturation. According to their known functions, it was possible to group the affected genes into three categories: regulators of hematopoiesis and lymphopoiesis; regulators of DNA replication, repair, and cell cycle; and regulators of pre-mRNA processing.

Regulators of Pre-mRNA Processing

The products of the five genes in the third functional group (*snapc3* [small nuclear RNA-activating *protein* complex protein 3], *lsm8* [like-Sm protein 8], *gemin5* [gem nuclear organelle associated *protein 5*], *tnpo3* [transportin 3], and *cstf3* [cleavage stimulation factor subunit 3]) are implicated in pre-mRNA processing. The mutations are predicted to affect different aspects of this multi-layered process, such as transcription of small nuclear RNAs (snRNAs) (*snapc3*) (Hernandez, 2001), formation of small nuclear RNA-containing ribonucleoprotein (snRNP) splicing complexes (*gemin5*; *lsm8*) (Friesen and Dreyfuss,

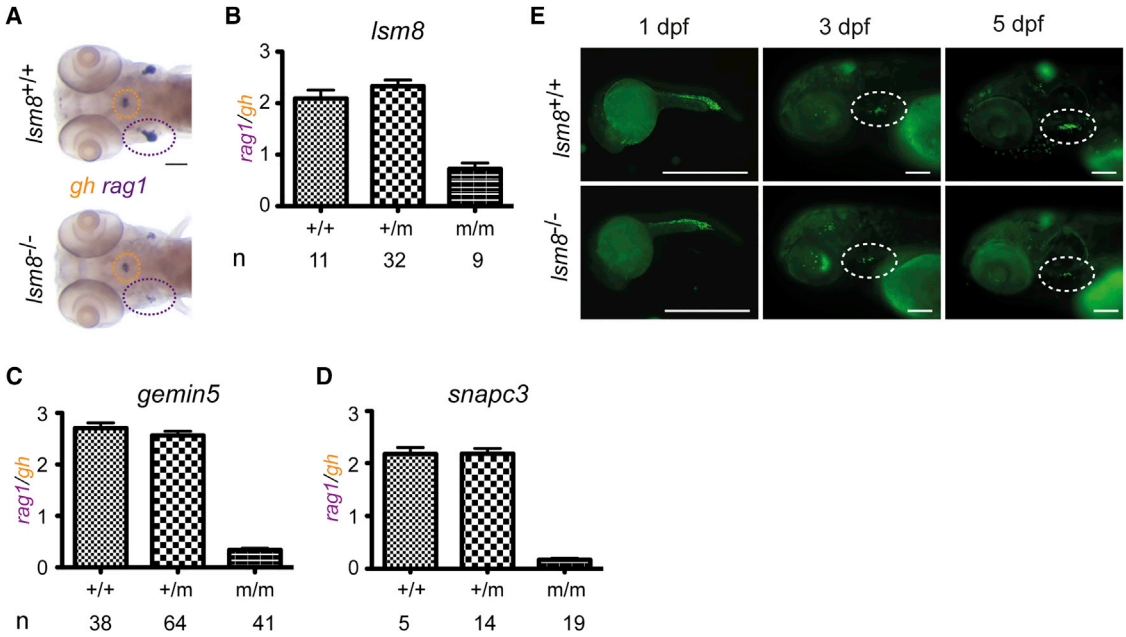

Figure 1. Impaired Early T Cell Development in Zebrafish Mutant for Genes Encoding Components of snRNPs, Related to Figures S1–S3

(A) Diagnostic whole-mount RNA in situ hybridization pattern in *lsm8* mutants using *rag1* (thymus encircled in purple), and *gh* (hypophysis encircled in orange) at 5 dpf. Scale bar, 10 μm.

(B–D) Quantification of the *rag1/gh* ratios as a measure of thymopoietic activity at 5 dpf. The number (n) of individual fish per genotype is indicated; mean ± SEM.

(E) In homozygous *lsm8* mutants (additionally transgenic for an *ikaros:eGFP* reporter), the number of *ikaros*-expressing cells in the thymus (encircled with dotted lines in middle and right panels) is drastically reduced at 5 dpf. Note the normal numbers of *ikaros*-positive cells in general hematopoietic tissues at 1 dpf. Scale bars, 100 μm.

2000), nuclear import of splice regulators (*tnpo3*) (Kataoka et al., 1999), and polyadenylation (*cstf3*) (Xiang et al., 2014). As our screen was focused on T cell development, the prevalence of this group of ubiquitously expressed genes was unexpected, particularly because, to the best of our knowledge, there is no precedence for their hematopoietic/lymphopoietic roles from studies in mammals. Previous biochemical studies indicated that the number of spliceosome-associated factors is in the order of 170 (Wahl et al., 2009), whereas the gene ontology term "RNA processing" is associated with about 500 genes. Assuming a coding capacity of the zebrafish genome of about 26,000 genes (Kettleborough et al., 2013), and using a conservative estimate that a total of 2,000 genes encode the various components of pre-mRNA-processing pathways, the degree of enrichment of genes in this functional category in our screen (5/15) is significant (hypergeometric test, $p = 0.0036$).

The unexpected prevalence of mutations in genes encoding components of the pre-mRNA-processing machinery in our screen prompted us to examine whether the cell-type-specific functions of the gene products of this group are mirrored in functional similarities, i.e., whether they belong to the same genetic network and whether their functions are evolutionarily conserved.

snRNP Function and T Cell Development

Despite the fact that the identified mutant alleles of *lsm8*, *gemin5*, and *snapc3* most likely encode non-functional variants, larval development and hematopoietic development initially proceed normally apart from a pronounced defect in T cell development (Figures S1–S3). We monitored the presence of developing T cells in the thymus of 5 dpf larvae by evaluating the signal emanating from *rag1*-expressing thymocytes in both thymic lobes; on a per-cell basis, *rag1* expression levels are the same in all genotypes analyzed, allowing us to use the *rag1* hybridization signal as a proxy for the number of *rag1*-expressing thymocytes. The signal emanating from growth hormone (*gh*) gene-expressing cells in the hypophysis was found to be unchanged in mutant fish and thus subsequently used as an internal standard (Figure 1A). The extent of T cell development was then expressed as the *rag1/gh* ratio and referred to as the thymopoietic index. The double-probe RNA in situ analyses indicate severe reductions of *rag1* signals in the thymic lobes of homozygous *lsm8*, *gemin5*, and *snapc3* mutants; heterozygotes exhibit no detectable decrease in the thymopoietic indices (Figures 1B–1D).

In contrast, other tissues in the developing larvae were much less affected. For example, in *lsm8* and *gemin5* mutants, the development of lymphoid precursors—visualized in the *ikaros:eGFP* transgenic background (Hess and Boehm, 2012)—is initially not affected (Figures 1E and 2A). However, by 5 dpf, fewer lymphoid precursors are present in the thymus—as identified by *ikaros* expression (Figures 1E and 2B), in line with the reduced *rag1* signal (Figures 1B, 1C, and 2C). By 8 dpf, T cell development in *gemin5*$^{-/-}$ fish has completely ceased (Figure 2D). This defect is lymphocyte intrinsic, because the stromal microenvironment of the thymus appears to be normal.

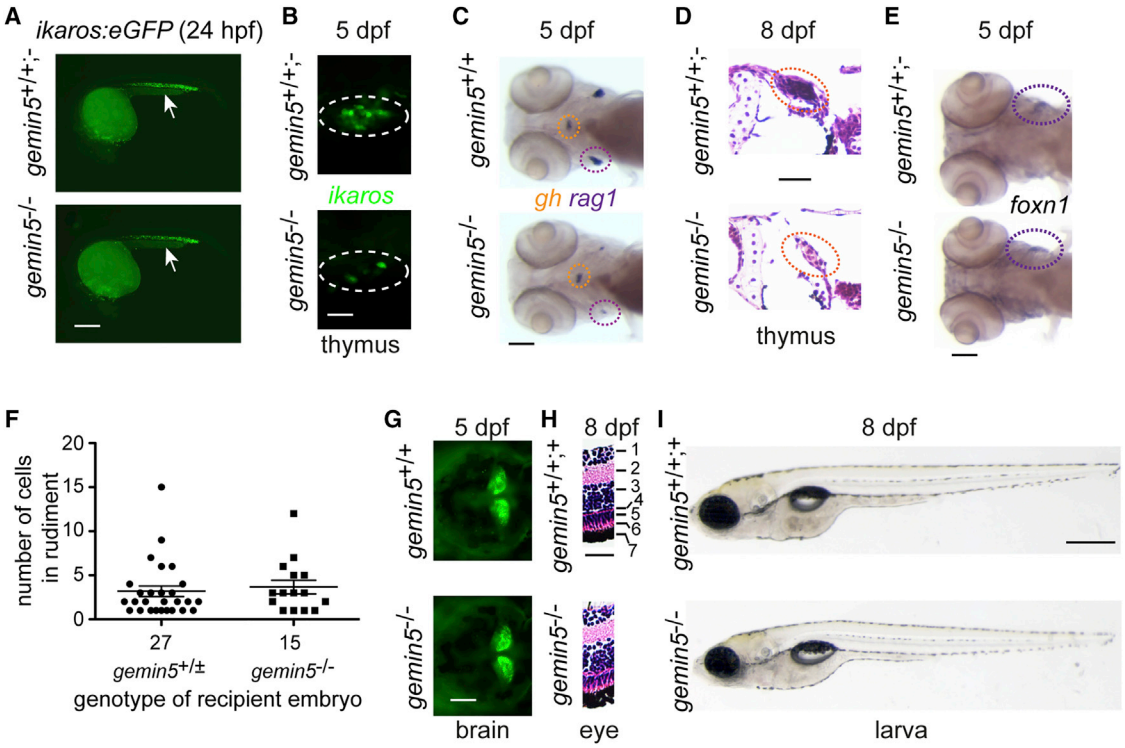

Figure 2. Tissue-Restricted Abnormalities in *gemin5* Mutants, Related to Figure S5

(A) Normal numbers and distribution of fluorescent lymphoid progenitor cells visualized in an *ikaros:eGFP* transgenic background (arrows). Scale bar, 10 μm.

(B) Reduced numbers of *ikaros*-expressing lymphocyte progenitors in the mutant thymus. Scale bar, 25 μm.

(C) Diagnostic whole-mount RNA in situ hybridization pattern in *gemin5* mutants using *rag1* (thymus encircled in purple), and *gh* (hypophysis encircled in orange) at 5 dpf. Scale bar, 100 μm.

(D) Lack of thymocytes in the thymus (red circle) at 8 dpf (H&E staining). Scale bar, 25 μm.

(E) Expression of the thymic epithelial marker *foxn1* (thymus encircled in purple) at 5 dpf. Scale bar, 100 μm.

(F) Normal receptive capacity of mutant thymic epithelium for whole kidney marrow hematopoietic cells isolated from adult wild-type *ikaros:eGFP* transgenic fish. At 5 dpf, the number of transplanted cells per embryo was determined. The overall success rate of the transplantation procedure is identical between the genotypes.

(G) Distribution of *ikaros*-expressing neurons in the mutant hindbrain. Scale bar, 100 μm.

(H) Retinal cell layers (1, ganglion cell layer; 2, inner plexiform layer; 3, inner nuclear layer; 4, outer plexiform layer; 5, outer nuclear layer; 6, photoreceptor cell layer; 7, retinal pigment epithelium) (right panel); H&E staining. Scale bar, 25 μm.

(I) Body size at 8 dpf. Scale bar, 500 μm.

No differences were observed for *gemin5*$^{+/+}$ and *gemin5*$^{+/-}$ fish for any of the analyzed parameters.

The mutant thymic anlage expresses *foxn1* (Figure 2E), the gene encoding the master regulator of thymic epithelial cell differentiation (Nehls et al., 1996), and is colonized normally by transplanted wild-type lymphoid precursors (Figure 2F). In contrast to impaired T cell development, several other features indicate that *gemin5*$^{-/-}$ embryos and larvae initially develop normally. For instance, development of different types of neuronal tissues appears undisturbed, including the hypophysis (exhibiting normal numbers of growth-hormone expressing cells [Figure 2C]), the hindbrain (visualized by *ikaros*-expressing neurons [Figure 2G]), and the retina (exhibiting the characteristic multilayered organization [Figure 2H]). Moreover, the swim bladder develops normally and the body size is indistinguishable from that of wild-type siblings [Figure 2I]). Collectively, these observations suggest a surprisingly tissue-restricted consequence of *gemin5* mutation during early stages of zebrafish development, well beyond the stages during which maternally supplied protein and/or mRNA could be expected to compensate for the loss of zygotic *gemin5* function. Likewise, fish mutant for *lsm8* (Figures 1 and S1) and *snapc3* (Figure S3) also exhibit tissue-restricted phenotypes.

Importantly, the phenotypes that are observed in pre-mRNA-processing mutants cannot be explained simply by impairment of the rapid cell proliferation occurring in developing zebrafish embryos and larvae, as this would also cause, for instance, severe perturbations in the development of cranio-facial and neuronal structures in addition to affecting T cell development. Rather, our findings point to a particular sensitivity of developing thymocytes to aberrations in certain components of snRNPs.

Epistasis Analysis

In order to gain insight into the functional interrelationships between the three regulators of pre-mRNA processing identified here, epistasis analysis was performed. The SMN (survival of

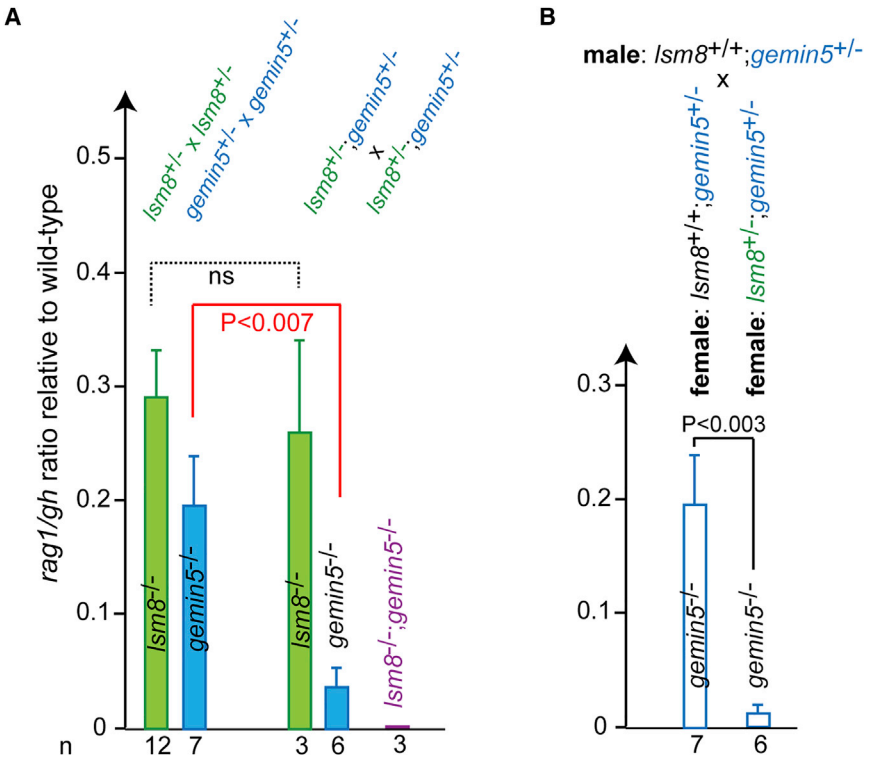

Figure 3. Epistasis between *lsm8* and *gemin5* Mutations, Related to Figure S4

(A and B) *lsm8* is a maternal effect gene resulting in synthetic interaction between *lsm8* and *gemin5*; the thymopoietic indices (*rag1/gh* ratio; mean values ± SD) at 5 dpf are given for fish (genotypes denoted in bars) resulting from crosses of parents whose genotypes and genders are indicated above the bars. The numbers of fish in each group are indicated.

motor neurons) complex (part of which is GEMIN5) contributes to the formation of U1, U2, U4, and U5 snRNPs, and to the formation of the spliceosomal U6 snRNP (containing the LSM2-8 protein ring) (Friesen and Dreyfuss, 2000). Hence, we tested whether genetic interaction was detectable between *gemin5* and *lsm8* mutations. Several features were notable. The phenotype of impaired intrathymic T cell development in *gemin5*$^{-/-}$ fish was considerably more severe when the fish originated from *gemin5*$^{+/-}$;*lms8*$^{+/-}$ double-heterozygous parents rather than from single heterozygous *gemin5*$^{+/-}$ (that is, *gemin5*$^{+/-}$;*lms8*$^{+/+}$) parents; by contrast, the phenotype of *lsm8*$^{-/-}$ fish was not affected by parental heterozygosity of *gemin5* (Figure 3A). The more severe phenotype of *gemin5* mutants arising from *lsm8* heterozygosity has a maternal origin (Figure 3B), suggesting that reduced levels of *lsm8* mRNA and/or protein in the oocyte affect the function of *gemin5* in the early stages of embryogenesis. By contrast, maternal contribution of *gemin5* mRNA and/or protein appears to be less important than that of *lsm8*, at least with respect to T cell development, because the extent of T cell development in *lsm8*$^{-/-}$ fish was unaffected by parental *gemin5* heterozygosity (Figure 3A). Impaired translation of maternal and zygotic *lsm8* mRNA (using antisense oligonucleotides directed against the translational start site) phenocopies the genetic *lsm8* defect and affects T cell development at later stages of development, whereas interference with splicing of zygotic *lsm8* pre-mRNAs alone (using antisense oligonucleotides directed against the splice donor site of exon 3), has no effect on the thymopoietic index (Figures S4A and S4B). Collectively, these observations indicate that reduced levels of LSM8 in the early embryo have a long-lasting effect that becomes apparent at much later stages of development and specifically affects T cell differentiation. Of note, the effect of maternal heterozygosity of *lsm8* was not observed in combination with a null mutation of the *il7r* gene, encoding a component of the il7 cytokine receptor (Figures S4C and S4D), which by itself also affects T cell development (Table 1) (Iwanami et al., 2011). Collectively, our observations support the notion that *gemin5* and *lsm8* function predominantly in separate pathways with redundant or complementary roles (Mani et al., 2008).

Epistasis analysis of *snapc3* mutants was complicated by the fact that their thymopoietic index is very low; hence, it proved to be difficult to establish by analysis of compound mutants the presence and the direction (synthetic or alleviating) of genetic interactions between *snapc3* and *lsm8* mutations and *snapc3* and *gemin5* (data not shown).

Perturbed Splicing Patterns in *snapc3* and *lsm8* Mutants

Next, we determined the effect of *snapc3* and *lsm8* mutations on the global splicing patterns in 4 dpf whole larvae using RNA sequencing (RNA-seq), as it is technically not feasible to isolate the few developing thymocytes for transcriptome analysis. The alterations of splicing patterns observed in both mutants are dominated by the occurrence of exon-skipping events (Figures 4A and 4B; Table S1). However, in *lsm8* mutants, a significant number of genes (including *tnpo3*) were additionally affected by incomplete splicing events, resulting in the frequent occurrence of retained introns (Figure 4B; Table S2). Other types of splicing events, such as the aberrant usage of mutually exclusive exons and the use of alternative donor and acceptor sites, did not appreciably contribute to the global changes in either genotype (Figures 4A and 4B). Intriguingly, we observed a considerable degree of overlap between the genes that are affected by splicing aberrations in the two mutants (Figures 4C and 4D; Tables S1 and S2). Interestingly, in *snapc3* mutant fish, skipping of the first coding exon of the *gemin8* gene (ENSDARG00000053496; ENSDART00000142315; Table S1; inclusion levels, 0.86 ± 0.05 [mean ± SEM] for wild type; 0.46 ± 0.02 [mean ± SEM] for mutant; p = 0.002; t test, two-tailed) was detected, predicting the formation of an N-terminally truncated protein. Because GEMIN8 is, like GEMIN5, part of the

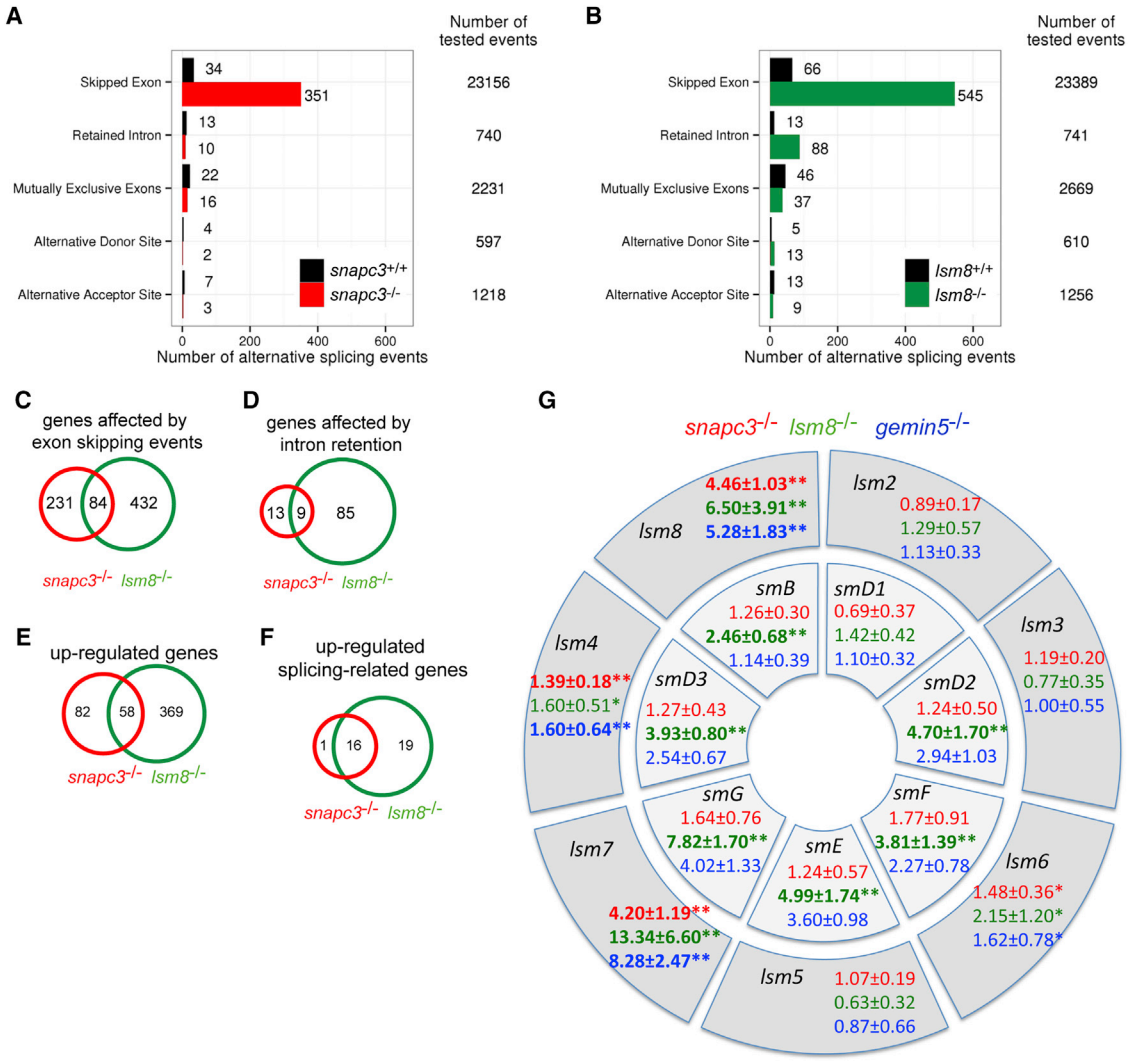

Figure 4. Aberrant Splicing Patterns in *snapc3* and *lsm8* Mutants

(A) Alternative splicing (AS) events in *snapc3* mutants at 4 dpf. Bar chart shows the number of significant AS events per condition at a false discovery rate (FDR) of 1% for five different AS event types. The total numbers of tested AS events are indicated on the right.

(B) AS events in *lsm8* mutants at 4 dpf.

(C) Genes commonly affected by alternative skipped exon events; in 72 of 84 instances, the same exon is affected.

(D) Genes commonly affected by intron retention; in 1 of 9 instances, the same intron is affected.

(E) Genes upregulated in the two genotypes.

(F) Genes whose products are implicated in pre-mRNA splicing upregulated in the two genotypes.

(G) Expression levels of genes (relative to wild type) encoding the components of the seven-membered SM and LSM rings of snRNP particles in mutant fish (see key for identification) at 5 dpf; results are depicted in a schematic of the seven-membered LSM and SM rings, with homologous proteins aligned. Mean expression values ± SD relative to *actin* as determined by qPCR; $n \geq 3$; t test, two-tailed: *$p < 0.05$; **$p < 0.01$.

SMN complex (Battle et al., 2006; Wahl et al., 2009), this observation supports the notion that *snapc3* and *gemin5* act in the same molecular pathway.

Changes in Gene Expression in *snapc3* and *lsm8* Mutants

To further address the functional consequences of the identified mutations, we also analyzed the transcriptomes of *snapc3* and *lsm8* mutants and their wild-type counterparts for changes in gene expression levels (≥2-fold; false discovery rate [FDR] < 5%) (Table S3). In *snapc3* mutants, 140 genes were significantly upregulated (Figure 4E), including 17 protein-coding genes with known functions in pre-mRNA splicing (Table S4). Most notable was the increase in expression levels for genes encoding components of the SM (*snrpa1*, *snrpd2*, *snrpd3*, *snrpe*, *snrpf*) and the LSM (*lsm7*, *lsm8*) heptameric complexes (Table S4). In *lsm8* mutants, the expression levels of 427 genes were increased (Figure 4E), including 35 protein-coding genes, the functions of which have been linked to pre-mRNA splicing (Table S4). As is the case in *snapc3* mutants, genes encoding components of

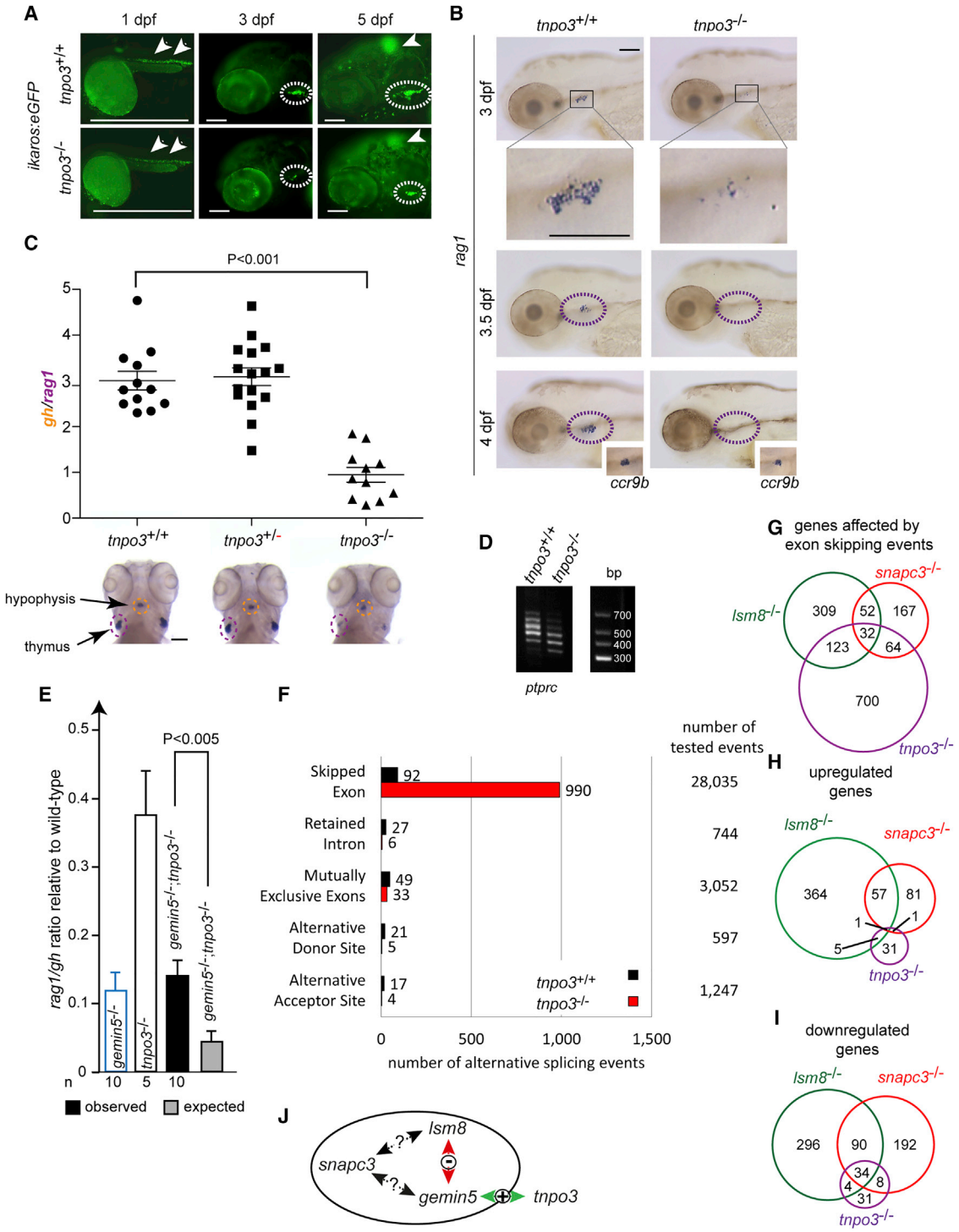

Figure 5. Characterization of *tnpo3* Mutants, Related to Figure S5

(A) Reduction of *ikaros*-expressing cells in the thymus (encircled with dotted lines in middle and right panels) of homozygous *tnpo3* mutants (additionally transgenic for an *ikaros:eGFP* reporter). Note the normal numbers of *ikaros*-positive cells in general hematopoietic tissues at 1 dpf. Scale bars, 100 μm.

(B) Maturation block of thymocytes. Few *ccr9b*-positive thymocytes (insets in 4 dpf panels) in *tnpo3* mutants express *rag1*. Scale bars, 100 μm.

(C) Thymopoietic indices at 5 dpf. Each symbol represents one animal. The mean ± SEM is indicated. Scale bar, 100 μm.

(D) Analysis of *ptprc* isoforms by RT-PCR; size markers are indicated.

(E) Masking genetic interaction between *gemin5* and *tnpo3* mutations in zebrafish. The thymopoietic indices (*rag1/gh* ratio; mean values ± SD) at 5 dpf are given for fish (genotypes denoted in bars) resulting from crosses of parents heterozygous for both *gemin5* and *tnpo3*; the observed thymopoietic index for

(legend continued on next page)

the SM (*snrpb*, *snrpd1*, *snrpd2*, *snrpd3*, *snrpe*, *snrpf*) and LSM (*lsm6*, *lsm7*, *lsm8*) ring structures are upregulated (Table S4). Of the 58 genes upregulated in both *snapc3* and *lsm8* mutants, 16 (28%) encode splicing-related proteins (Figure 4F). This includes *snapc4*, encoding one component of the transcriptional activation complex of snRNA genes, and of genes (*snrpd2*, *snrpd3*, *snrpe*, *snrpf*, *lsm7*, *lsm8*) encoding 6 of the 14 components of the SM and LSM heptameric ring structures containing snRNAs (Table S4). In both *lsm8* and *snapc3* mutants, expression of the *foxg1d* gene is reduced (Table S3); the mouse homolog of this gene (*Foxg1*) is implicated in the regulation of thymic epithelial cell differentiation (Wei and Condie, 2011), possibly contributing to impaired T cell development.

We then tested the generality of the presumed transcriptional feedback regulation among components of snRNPs by examining transcriptional responses in *gemin5* mutants, focusing on the expression levels of *sm* and *lsm* genes. In support of our hypothesis, the qPCR results indicate that *snapc3*, *lsm8*, and *gemin5* mutations all result in strong upregulation of *lsm7* and *lsm8* mRNAs (Figure 4G), defining a core group of genes co-regulated by perturbation of *snapc3*, *lsm8*, and *gemin5* functions. By contrast, expression levels of mRNAs of genes encoding the eight known GEMIN protein family members are largely unaffected in the three mutants (Table S5), supporting the notion of the specific nature of the transcriptional feedback regulation. Collectively, the present genetic interaction studies and transcriptome analyses suggest the presence of a network connecting *snapc3*, *lsm8*, and *gemin5* genes encoding key components of snRNPs that appears to converge on the transcriptional regulation of *lsm7* and *lsm8* genes.

tnpo3 As a Regulator of Early T Cell Development in Zebrafish

TNPO3 has been shown to participate in the import of splice regulators to the nucleoplasm (Maertens et al., 2014). Hence, in contrast to the gene products of *snapc3*, *lsm8*, and *gemin5*, TNPO3 is predicted to indirectly affect pre-mRNA processing. In zebrafish *tnpo3* mutant larvae, the number of lymphoid precursors in hematopoietic tissues is not affected at 1 dpf when definitive hematopoiesis has begun in zebrafish; at later stages of development, lymphoid progenitors are found in the thymus (albeit in somewhat reduced numbers), indicating that the homing process is largely unaffected by *tnpo3* deficiency (Figures 5A and S5). However, only few of thymocytes in *tnpo3* mutants express *rag1* (Figures 5B and 5C), despite normal expression levels of a thymocyte marker, *ccr9b* (Figure 5B), suggesting that intrathymic defects contribute to impaired T cell development in *tnpo3*-deficient fish. At the time point of our analyses (5 dpf), only T cells are present in zebrafish larvae, because B cells develop considerably later in development (Danilova and Steiner, 2002). Hence, we reasoned that the splicing pattern of *ptprc* (encoding the zebrafish ortholog of the mammalian thymocyte maturation marker CD45) might provide further evidence for impaired intrathymic T cell differentiation in *tnpo3*-deficient larvae. Indeed, the mutant splicing pattern is dominated by lower molecular weight isoforms (Figure 5D) that are characteristically found in immature mouse thymocytes (Lefrancois and Goodman, 1987). At present, it is not possible to determine the cause-and-effect relationship of differential *ptprc* splicing in the absence of TNPO3 function. However, *tnpo3*-deficient zebrafish larvae exhibit aberrant splicing of the *nck2b* gene (Table S1), encoding the zebrafish homolog of the essential adaptor protein NCK required for proper TCR signaling in the mouse (Alarcón et al., 2003), suggesting that differential splicing of *ptprc* is an indirect effect of *tnpo3* deficiency.

tnpo3 appears to be functionally connected to the *snpac3*/*lsm8*/*gemin5* network of splice regulators, as indicated by alleviating genetic interaction between *tnpo3* and *gemin5* mutations. In double-deficient fish, the thymopoietic index is lower than in each of the single mutants, yet 3-fold higher than expected if the two genes acted independently (Mani et al., 2008) (Figure 5E), suggesting that *tnpo3* and *gemin5* are active in the same pathway. As expected, splicing defects were abundant in 4 dpf *tnpo3* mutants possibly owing to faulty transport of splice regulators to the nucleoplasm (Maertens et al., 2014). We recorded a considerably greater number of exon-skipping events in mutant fish compared to their wild-type siblings, alongside other splicing changes, such as the presence of retained introns and the use of mutually exclusive exons or alternative splice donor and splice acceptor sites (Figures 5F and 5G; Tables S1 and S2). Interestingly, we observed that both *lsm8* and *tnpo3* deficiency are associated with aberrant splicing of *gemin5* and *tnpo3* pre-mRNA, and *snapc3*- and *tnpo3*-deficient larvae both exhibit aberrant splicing patterns of *gemin8* (Table S1), further emphasizing the functional interrelationships in the *snpac3*/*lsm8*/*gemin5*/*tnpo3* network.

Comparatively few alterations were observed at the level of gene expression ($\geq$2-fold; FDR < 5% [Table S3]) in *tnpo3* mutants. Thirty-eight genes are upregulated in *tnpo3* mutants, however, with little overlap to genes upregulated in *snapc3* and *lsm8* mutants, indicating the presence of mechanistic differences with respect to the regulation of snRNP assembly among the three mutants (Figure 5H).

Changes in Transcriptomes Common to *snpac3*, *lsm8*, and *tnpo3* Mutants

The presence of pervasive autoregulation affecting the processing of pre-mRNAs of splice regulator genes as a consequence of

gemin5$^{-/-}$;*tnpo3*$^{-/-}$ double mutants is significantly higher than that expected from the indices of single mutants under the multiplicative model of genetic interaction. The numbers of fish in each group is indicated.

(F) Alternative splicing events in *tnpo3* mutants at 4 dpf. Bar chart shows the number of significant AS events per condition at a false discovery rate (FDR) of 1% for five different AS event types. The total numbers of tested AS events are indicated on the right.

(G) Genes affected by exon-skipping events.

(H) Genes exhibiting transcriptional upregulation.

(I) Genes exhibiting transcriptional downregulation.

(J) Summary of the network structure involving *snapc3*, *lsm8*, *gemin5*, and *tnpo3* genes. +, alleviating genetic interaction; −, synthetic interaction; ?, unclear.

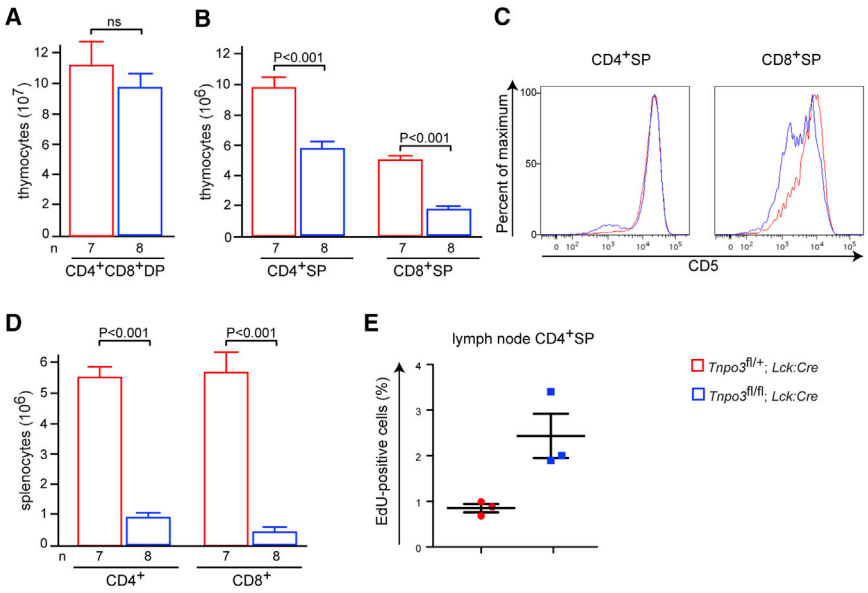

Figure 6. Characterization of Conditional Mouse *Tnpo3* Mutants, Related to Figure S6

(A) Absolute numbers of $CD4^+CD8^+$ double-positive (DP) cells per thymus (mean ± SEM).

(B) Absolute numbers $CD4^+$ and $CD8^+$ single-positive (SP) thymocytes (mean ± SEM).

(C) CD5 surface levels on single-positive thymocytes; panels representative of three biological replicates.

(D) Numbers of peripheral $CD4^+$ and $CD8^+$ single-positive T cells in *Tnpo3*-deficient mice (mean ± SEM).

(E) Proliferation of peripheral T cells (exemplified by $CD4^+$ lymph node cells).

mutations in *snpac3*, *lsm8*, and *tnpo3* is suggested by our finding that among the 32 genes commonly affected by exon-skipping events (Figure 5G), two genes—*srsf3a* and *ptbp3*—encode known regulators of pre-mRNA processing; and of the four genes commonly affected by intron retention, two encode splice regulators (*srsf1b*, *prpf39*) (Table S2).

When we examined transcriptomes for changes common to all three mutants and potentially involved in T cell/thymus development, we noted that splicing of the *dnmt4* (also known as *dnmt3bb.1*) gene, which is expressed in the hematopoietic lineage (Takayama et al., 2014), is similarly affected in all three mutants; the splice pattern suggests the presence of different compositions of the N-terminal non-catalytic domains of the predicted protein (Figure 5G; Table S6).

Many of the 34 downregulated genes (Figure 5I) are signature genes of the exocrine pancreas, identifying a second cell type exhibiting particular sensitivity to the malfunction of the pre-mRNA splicing regulators identified here. The lower expression levels of elastase, trypsin, amylase, and carboxypeptidase, etc. (*ela3l*, *try*, *amy2a*, *cpa1*) genes suggest that the downstream effects of *snapc3*, *lsm8*, and *tnpo3* mutations converge on malfunction of the exocrine pancreas (Table S7). This conclusion is supported by the fact that in all three mutants, aberrant splicing of the NR5A2 transcription factor also occurs (Table S6), which is required for liver and exocrine pancreas development (Nissim et al., 2016). We also note that the gene encoding the brush-border membrane glycoprotein Trehalase (*treh*) is affected by intron retention in all three mutants, adding to impaired absorption of carbohydrates. Although more work is needed to assess the functional significance of these findings, we hypothesize that malfunction of the exocrine pancreas and the intestine at least partly underlies the phenotype of premature death in the mutant fish. These results also underscore the notion of cell-type-restricted functions of *snapc3*, *lsm8*, and *tnpo3* genes.

Tnpo3 Deficiency in Mouse T Cells

Having established the role of the *snpac3/lsm8/gemin5/tnpo3* network (Figure 5J) in zebrafish T cell development, we next examined a possible evolutionary conservation of functions of these genes in mammalian T cell development; we chose the mouse *Tnpo3* gene for our studies. To this end, we generated conditional knockout mice using a floxed allele of *Tnpo3* (exon 7 is flanked by *lox*P sites) and *Lck:Cre* (Orban et al., 1992) to eliminate *Tnpo3* in the αβ lineage of T cells. Under these conditions, complete inactivation of the *Tnpo3* gene was achieved (Figure S6). The predicted TNPO3 mutant protein consisting of the first 291 amino acids closely resembles the mutant form identified in zebrafish (202 amino acids) (Figure S6); notably, they both lack the region required for interaction with RS cargo proteins (Maertens et al., 2014). In the thymus, *Tnpo3* deficiency was accompanied by a moderate, but non-significant reduction of CD4/CD8-double-positive (DP) T cell progenitors; by contrast, single-positive (SP) thymocytes were significantly reduced, $CD4^+$ cells by about 40% and $CD8^+$ cells by about 60% (Figures 6A and 6B). As expected, the number of γδ T cells remained unchanged, because the *Lck:Cre* transgene is not expressed in this lineage (Figure S6). Reduced levels of CD5 staining of *Tnpo3*-deficient αβ thymocytes (particularly of those with $CD8^+$ surface phenotype) indicate that TCR signaling is impaired in mutant cells (Figure 6C); this feature is also evident in peripheral T cells (Figure S6). These findings suggest that loss of *Tnpo3* in thymocytes is associated with an incomplete maturation block affecting the DP-to-SP transition. Because expression levels of *Rag* genes are unchanged in mutant DP cells (data not shown), we attribute the mutant phenotype to impaired TCR signaling. This finding is reminiscent of the features of impaired TCR signaling identified in the *tnpo3*-deficient zebrafish larvae. The loss of single-positive cells in mutant thymi does not appear to be due to increased apoptosis, because the fractions of TUNEL-positive and Annexin V-positive thymocytes remained unchanged (data not shown); these findings call for further mechanistic studies addressing migration, survival, etc., of mutant T cells in the periphery. As expected for the lymphopenic condition in *Tnpo3*-deficient mice (Figure 6D), increased proliferation levels of peripheral T cells are observed (Figure 6E), compatible with the notion that TNPO3 deficiency per se does not impair cell proliferation.

Collectively, the present data suggest an evolutionarily conserved role of TNPO3 in T cell differentiation.

DISCUSSION

Our unbiased genetic screens identified an extended genetic network linking genes of several distinct functional categories (hematopoietic differentiation; DNA replication/repair; pre-mRNA processing) required for early stages of intrathymic T cell development in zebrafish. The present study has established additional animal models for mammalian (particularly human) immunodeficiency syndromes and presents previously unknown candidate genes whose mutations might underlie failing immune function. Indeed, we note that some of the genes that we have identified are implicated in human immunodeficiency disorders, such as *il7r* (Puel et al., 1998), *jak3* (Russell et al., 1995), and *pole1* (Pachlopnik Schmid et al., 2012) (Table 1). The value of forward genetic screens to identify candidate genes is underscored by our finding of an enrichment of genes encoding factors involved in pre-mRNA processing. This outcome was unexpected, because mutations in this group of genes have so far been associated mostly with neuronal disease, such as spinal muscular atrophy or retinitis pigmentosa (Singh and Cooper, 2012). Mutations in spliceosomal factors manifest themselves as hypomorphic alleles (Singh and Cooper, 2012), indicating that the resulting phenotypes most likely arise from subtle perturbations in the multi-component protein complexes regulating pre-mRNA splicing. For example, insufficient levels of the SMN complex are associated with impaired maturation of snRNPs and aberrant splicing reactions in neuronal tissues (Zhang et al., 2008, 2013), whereas complete loss of SMN function is lethal (Hsieh-Li et al., 2000). However, because defects in early development are buffered by maternal factors, our results also illustrate how the unique biological features of the zebrafish model allow the identification of tissue-restricted functions of pleiotropic genes also in the case of null alleles, which in the mammalian system can only be studied by conditional mutagenesis.

Although the results of the present epistasis analysis are consistent with those in previously published molecular studies on snRNP assembly and function (Wahl et al., 2009), an unexpected finding in the in vivo studies described here is the presence of a feedback loop connecting impaired *snapc3*, *lsm8*, and *gemin5* function with the transcriptional regulation of the *lsm7* and *lsm8* genes. In contrast to many other genes in zebrafish, *lsm* genes do not possess paralogs. Hence, the transcriptional response in our mutants is unlikely to be part of a direct compensatory mechanism, but rather appears to be a general consequence of snRNP biogenesis perturbation, because expression levels of *lsm7* and *lsm8* are also upregulated in zebrafish larvae mutant for the p110 splicing regulator (Trede et al., 2007), which is required for recycling of the U4/U6 snRNP from singular U4 and U6 snRNPs (Bell et al., 2002). Another notable feature of transcriptional changes emerging from our studies is the presence of pervasive autoregulatory loops affecting the splicing of pre-mRNAs-encoding splice regulators, as illustrated here by, for instance, the *srsf3a* gene, a homolog of the mammalian *Srsf3* gene previously shown to be regulated by variable inclusion of so-called poison-cassette exons (Lareau et al., 2007). On a more general level, our findings provide evidence for the emerging notion of tissue-restricted roles played by ubiquitous components of basic cellular pathways. Future work may thus reveal an ''RNA splicing code'' of context- and cell-type-dependent functions of some general-purpose factors involved in pre-mRNA processing; our mutants provide an entry point into the identification of the precise mechanism(s) by which pre-mRNA splicing affects T cell development.

With respect to the mechanism(s) underlying failing T cell development in zebrafish larvae, our work indicates that, despite mechanistic differences, certain commonalities exist among the aberrations caused by mutations in the *snapc3/lsm8/gemin5/tnpo3* network. One particularly notable observation is the apparent association with DNA methylation, because the splicing of several genes encoding putative de novo DNA methylases is affected by perturbations in this network; most importantly, aberrant processing of the *dnmt3bb.1* gene is a common feature of *snapc3*, *lsm8*, and *tnpo3* mutants. We consider this mechanistic link to be particularly intriguing, because our screen has independently uncovered a missense mutation in the gene encoding the maintenance DNA methylase *dnmt1* (Table 1). Given that the status of DNA methylation affects the differentiation of hematopoietic stem cells (Challen et al., 2014) and modulates immune functions including T cell differentiation (Jin et al., 2008), it will be interesting to examine the possible presence of common changes in gene-specific DNA methylation patterns to identify those genes whose methylation signatures are crucial to normal T cell development.

Finally, an important aspect of our present work addresses the evolutionarily conserved function of the identified network of splice regulators with respect to T cell differentiation. We chose TNPO3 to verify that the observations made in the zebrafish model also hold for the mammalian system. Our conditional mouse *Tnpo3* knockout model exhibits a phenotype of impaired T cell differentiation, resembling the phenotype observed in *tnpo3*-deficient zebrafish larvae. The comparative analysis of mutant zebrafish *tnpo3* and mouse *Tnpo3* genes highlights the advantages of the zebrafish model to identify cell-type-restricted functions of pleiotropic regulators, because *Tnpo3*-deficient mice exhibit early embryonic lethality. Future work will have to be aimed at addressing the degree of functional conservation for the other members of the identified genetic networks and the precise molecular mechanism(s) underlying the exquisite sensitivity of T cells to perturbed pre-mRNA splicing.

EXPERIMENTAL PROCEDURES

Animals

The zebrafish (*Danio rerio*) strains Ekkwill (EKK), Tüpfel long fin (TL), wild-type-in-Kalkutta (WIK), AB, Assam (ASS), and Tübingen (TÜ) are maintained in the animal facility of the Max Planck Institute of Immunobiology and Epigenetics. The *ikaros:eGFP* transgenic line was described previously (Hess and Boehm, 2012). The floxed *Tnpo3* allele of the mouse was maintained on the C57BL/6J background. All animal experiments were approved by the institute's review committee and conducted under licenses from the local government (Regierungspräsidium Freiburg).

ENU Mutagenesis of Zebrafish and Mutant Recovery

A detailed description of the screen design, coverage, complementation analysis, and mutant identification by positional cloning and whole genome sequencing can be found in Supplemental Experimental Procedures.

Tnpo3 Conditional Knockout Mice

The ESC line EPD0318_3_G02 (genetic background: C57BL/6N Agouti(A/a); allele name: *Tnpo3*$^{tm1a(KOMP)Wtsi}$) was obtained from the KOMP Repository and used to derive chimeric mice using standard procedures.

Morphants and Phenotypic Rescue

Morphants were generated as described (Schorpp et al., 2006). For rescue experiments, mRNAs were injected into fertilized eggs and analysis carried out by *gh* and *rag1* RNA in situ hybridization at various time points after injection.

Cell Transplantation and Live Microscopy

EGFP$^+$ cells were sorted from single-cell suspensions of kidney marrow cells isolated from adult *ikaros:eGFP* transgenic zebrafish and injected into the sinus venosus of embryos from heterozygous intercrosses at 2 dpf. GFP$^+$ cells in the thymic region were counted using Imager.Z1 (Zeiss) at 3 days post-injection. The procedures for live imaging using the *ikaros:eGFP* transgenic background were described previously (Hess and Boehm, 2012).

Flow Cytometry

For analysis of *Tnpo3* mutant mice, analytical flow cytometry was carried out as described in Calderón and Boehm (2012).

RNA In Situ Hybridization

Procedures for RNA in situ hybridization and probes were described previously (Schorpp et al., 2006). The determination of *rag1*/*gh* ratios was carried out as described in Supplemental Experimental Procedures.

RNA Extraction, cDNA Synthesis, and qPCR

Total RNA was extracted using TRI Reagent (Sigma) following the manufacturer's instructions. After treatment with Cloned DNaseI (Takara), RNA extraction using TRI Reagent was repeated. Superscript II Reverse Transcriptase (Invitrogen) and random hexamer primers were used for cDNA synthesis from total RNA. qPCR was carried out as described (Rode and Boehm, 2012); primers are listed in Table S8.

RNA Sequencing and Computational Analysis of RNA-Seq Data

Total RNA was extracted from whole zebrafish larvae at 4 dpf and subjected to transcriptome analysis. The libraries were sequenced in paired-end 75-bp mode on 0.8 lanes per sample on an Illumina HiSeq 2500 instrument. The high-throughput RNA sequencing analysis pipeline, version 0.4.2, written by Fabian Kilpert (https://github.com/kilpert/rna-seq-qc) was applied as described in Supplemental Experimental Procedures. RNA-seq data are deposited in NCBI's GEO (Edgar et al., 2002) and are accessible through GEO: GSE77480.

Statistics

For single comparisons of independent groups, Student's t test or the Mann-Whitney test was performed depending on the sample size and distribution. Analyses were performed using Prism software. The statistical models applied to RNA-seq data are described in Supplemental Experimental Procedures.

ACCESSION NUMBERS

The accession number for the RNA-seq data reported in this paper is GEO: GSE77480.

SUPPLEMENTAL INFORMATION

Supplemental Information includes Supplemental Experimental Procedures, six figures, and eight tables and can be found with this article online at http://dx.doi.org/10.1016/j.celrep.2016.11.003.

AUTHOR CONTRIBUTIONS

N.I., M.M., L.G., C.S.-R., D.-F.L., F.M., and M.S. identified and characterized zebrafish mutants by positional cloning. N.I., M.M., L.G., C.S.-R., D.-F.L., I.H., C.P.O., and M.S. determined the phenotypes of zebrafish mutants. N.I. established and characterized the *Tnpo3*-mutant mice. K.S. and A.S.R. carried out the bioinformatic analysis of RNA-seq data. N.I, M.S., and T.B. conceived and designed the study. N. I. and T.B. wrote the paper. N.I., K.S., A.S.R., M.M., L.G., C.S.-R., D.-F.L., F.M., I.H., C.P.O., M.S., and T.B. contributed to the writing of the manuscript.

ACKNOWLEDGMENTS

This project has received funding from the Max Planck Society and the European Research Council under the European Union's Seventh Framework Programme (FP7/2007–2013) ERC Grant Agreement 323126. The mutant screen was conducted in collaboration with the Tübingen 2000 Screen Consortium and the Freiburg Screening Group; their members are listed in Supplemental Experimental Procedures. We thank W. Wiest for initial identification of the WW18/10 mutant, B. Kanzler for help in the establishment of the mouse *Tnpo3* mutant, D. Bönsch for excellent animal care, and U. Bönisch, E. Betancourt, and S. Diehl for help with next-generation sequencing.

Received: April 24, 2016
Revised: September 5, 2016
Accepted: October 25, 2016
Published: November 22, 2016

REFERENCES

Alarcón, B., Gil, D., Delgado, P., and Schamel, W.W. (2003). Initiation of TCR signaling: regulation within CD3 dimers. Immunol. Rev. *191*, 38–46.

Battle, D.J., Lau, C.-K., Wan, L., Deng, H., Lotti, F., and Dreyfuss, G. (2006). The Gemin5 protein of the SMN complex identifies snRNAs. Mol. Cell *23*, 273–279.

Bell, M., Schreiner, S., Damianov, A., Reddy, R., and Bindereif, A. (2002). p110, a novel human U6 snRNP protein and U4/U6 snRNP recycling factor. EMBO J. *21*, 2724–2735.

Boehm, T. (2011). Design principles of adaptive immune systems. Nat. Rev. Immunol. *11*, 307–317.

Boehm, T., Bleul, C.C., and Schorpp, M. (2003). Genetic dissection of thymus development in mouse and zebrafish. Immunol. Rev. *195*, 15–27.

Calderón, L., and Boehm, T. (2012). Synergistic, context-dependent, and hierarchical functions of epithelial components in thymic microenvironments. Cell *149*, 159–172.

Challen, G.A., Sun, D., Mayle, A., Jeong, M., Luo, M., Rodriguez, B., Mallaney, C., Celik, H., Yang, L., Xia, Z., et al. (2014). Dnmt3a and Dnmt3b have overlapping and distinct functions in hematopoietic stem cells. Cell Stem Cell *15*, 350–364.

Danilova, N., and Steiner, L.A. (2002). B cells develop in the zebrafish pancreas. Proc. Natl. Acad. Sci. USA *99*, 13711–13716.

den Dunnen, J.T., and Antonarakis, S.E. (2000). Mutation nomenclature extensions and suggestions to describe complex mutations: a discussion. Hum. Mutat. *15*, 7–12.

Edgar, R., Domrachev, M., and Lash, A.E. (2002). Gene Expression Omnibus: NCBI gene expression and hybridization array data repository. Nucleic Acids Res. *30*, 207–210.

Friesen, W.J., and Dreyfuss, G. (2000). Specific sequences of the Sm and Sm-like (Lsm) proteins mediate their interaction with the spinal muscular atrophy disease gene product (SMN). J. Biol. Chem. *275*, 26370–26375.

Hernandez, N. (2001). Small nuclear RNA genes: a model system to study fundamental mechanisms of transcription. J. Biol. Chem. *276*, 26733–26736.

Hess, I., and Boehm, T. (2012). Intravital imaging of thymopoiesis reveals dynamic lympho-epithelial interactions. Immunity *36*, 298–309.

Hirano, M., Guo, P., McCurley, N., Schorpp, M., Das, S., Boehm, T., and Cooper, M.D. (2013). Evolutionary implications of a third lymphocyte lineage in lampreys. Nature *501*, 435–438.

Hsieh-Li, H.M., Chang, J.-G., Jong, Y.-J., Wu, M.-H., Wang, N.M., Tsai, C.H., and Li, H. (2000). A mouse model for spinal muscular atrophy. Nat. Genet. *24*, 66–70.

Iwanami, N., Mateos, F., Hess, I., Riffel, N., Soza-Ried, C., Schorpp, M., and Boehm, T. (2011). Genetic evidence for an evolutionarily conserved role of IL-7 signaling in T cell development of zebrafish. J. Immunol. *186*, 7060–7066.

Jin, B., Tao, Q., Peng, J., Soo, H.M., Wu, W., Ying, J., Fields, C.R., Delmas, A.L., Liu, X., Qiu, J., and Robertson, K.D. (2008). DNA methyltransferase 3B (DNMT3B) mutations in ICF syndrome lead to altered epigenetic modifications and aberrant expression of genes regulating development, neurogenesis and immune function. Hum. Mol. Genet. *17*, 690–709.

Kataoka, N., Bachorik, J.L., and Dreyfuss, G. (1999). Transportin-SR, a nuclear import receptor for SR proteins. J. Cell Biol. *145*, 1145–1152.

Kettleborough, R.N.W., Busch-Nentwich, E.M., Harvey, S.A., Dooley, C.M., de Bruijn, E., van Eeden, F., Sealy, I., White, R.J., Herd, C., Nijman, I.J., et al. (2013). A systematic genome-wide analysis of zebrafish protein-coding gene function. Nature *496*, 494–497.

Langenau, D.M., and Zon, L.I. (2005). The zebrafish: a new model of T-cell and thymic development. Nat. Rev. Immunol. *5*, 307–317.

Lareau, L.F., Inada, M., Green, R.E., Wengrod, J.C., and Brenner, S.E. (2007). Unproductive splicing of SR genes associated with highly conserved and ultra-conserved DNA elements. Nature *446*, 926–929.

Lefrancois, L., and Goodman, T. (1987). Developmental sequence of T200 antigen modifications in murine T cells. J. Immunol. *139*, 3718–3724.

Maertens, G.N., Cook, N.J., Wang, W., Hare, S., Gupta, S.S., Öztop, I., Lee, K., Pye, V.E., Cosnefroy, O., Snijders, A.P., et al. (2014). Structural basis for nuclear import of splicing factors by human Transportin 3. Proc. Natl. Acad. Sci. USA *111*, 2728–2733.

Mani, R., St Onge, R.P., Hartman, J.L., 4th, Giaever, G., and Roth, F.P. (2008). Defining genetic interaction. Proc. Natl. Acad. Sci. USA *105*, 3461–3466.

Mönnich, M., Hess, I., Wiest, W., Bachrati, C., Hickson, I.D., Schorpp, M., and Boehm, T. (2010). Developing T lymphocytes are uniquely sensitive to a lack of topoisomerase III alpha. Eur. J. Immunol. *40*, 2379–2384.

Nehls, M., Kyewski, B., Messerle, M., Waldschütz, R., Schüddekopf, K., Smith, A.J., and Boehm, T. (1996). Two genetically separable steps in the differentiation of thymic epithelium. Science *272*, 886–889.

Nissim, S., Weeks, O., Talbot, J.C., Hedgepeth, J.W., Wucherpfennig, J., Schatzman-Bone, S., Swinburne, I., Cortes, M., Alexa, K., Megason, S., et al. (2016). Iterative use of nuclear receptor Nr5a2 regulates multiple stages of liver and pancreas development. Dev. Biol. *418*, 108–123.

Orban, P.C., Chui, D., and Marth, J.D. (1992). Tissue- and site-specific DNA recombination in transgenic mice. Proc. Natl. Acad. Sci. USA *89*, 6861–6865.

Pachlopnik Schmid, J., Lemoine, R., Nehme, N., Cormier-Daire, V., Revy, P., Debeurme, F., Debré, M., Nitschke, P., Bole-Feysot, C., Legeai-Mallet, L., et al. (2012). Polymerase ε1 mutation in a human syndrome with facial dysmorphism, immunodeficiency, livedo, and short stature ("FILS syndrome"). J. Exp. Med. *209*, 2323–2330.

Pandolfi, P.P., Roth, M.E., Karis, A., Leonard, M.W., Dzierzak, E., Grosveld, F.G., Engel, J.D., and Lindenbaum, M.H. (1995). Targeted disruption of the *GATA3* gene causes severe abnormalities in the nervous system and in fetal liver haematopoiesis. Nat. Genet. *11*, 40–44.

Puel, A., Ziegler, S.F., Buckley, R.H., and Leonard, W.J. (1998). Defective *IL7R* expression in $T^{-}B^{+}NK^{+}$ severe combined immunodeficiency. Nat. Genet. *20*, 394–397.

Rode, I., and Boehm, T. (2012). Regenerative capacity of adult cortical thymic epithelial cells. Proc. Natl. Acad. Sci. USA *109*, 3463–3468.

Russell, S.M., Tayebi, N., Nakajima, H., Riedy, M.C., Roberts, J.L., Aman, M.J., Migone, T.-S., Noguchi, M., Markert, M.L., Buckley, R.H., et al. (1995). Mutation of Jak3 in a patient with SCID: essential role of Jak3 in lymphoid development. Science *270*, 797–800.

Schorpp, M., Bialecki, M., Diekhoff, D., Walderich, B., Odenthal, J., Maischein, H.-M., Zapata, A.G., and Boehm, T. (2006). Conserved functions of Ikaros in vertebrate lymphocyte development: genetic evidence for distinct larval and adult phases of T cell development and two lineages of B cells in zebrafish. J. Immunol. *177*, 2463–2476.

Singh, R.K., and Cooper, T.A. (2012). Pre-mRNA splicing in disease and therapeutics. Trends Mol. Med. *18*, 472–482.

Soza-Ried, C., Hess, I., Netuschil, N., Schorpp, M., and Boehm, T. (2010). Essential role of *c-myb* in definitive hematopoiesis is evolutionarily conserved. Proc. Natl. Acad. Sci. USA *107*, 17304–17308.

Takayama, K., Shimoda, N., Takanaga, S., Hozumi, S., and Kikuchi, Y. (2014). Expression patterns of *dnmt3aa*, *dnmt3ab*, and *dnmt4* during development and fin regeneration in zebrafish. Gene Expr. Patterns *14*, 105–110.

Trede, N.S., Medenbach, J., Damianov, A., Hung, L.H., Weber, G.J., Paw, B.H., Zhou, Y., Hersey, C., Zapata, A., Keefe, M., et al. (2007). Network of coregulated spliceosome components revealed by zebrafish mutant in recycling factor p110. Proc. Natl. Acad. Sci. USA *104*, 6608–6613.

Wahl, M.C., Will, C.L., and Lührmann, R. (2009). The spliceosome: design principles of a dynamic RNP machine. Cell *136*, 701–718.

Wei, Q., and Condie, B.G. (2011). A focused in situ hybridization screen identifies candidate transcriptional regulators of thymic epithelial cell development and function. PLoS One *6*, e26795.

Xiang, K., Tong, L., and Manley, J.L. (2014). Delineating the structural blueprint of the pre-mRNA 3′-end processing machinery. Mol. Cell. Biol. *34*, 1894–1910.

Yui, M.A., and Rothenberg, E.V. (2014). Developmental gene networks: a triathlon on the course to T cell identity. Nat. Rev. Immunol. *14*, 529–545.

Zhang, Z., Lotti, F., Dittmar, K., Younis, I., Wan, L., Kasim, M., and Dreyfuss, G. (2008). SMN deficiency causes tissue-specific perturbations in the repertoire of snRNAs and widespread defects in splicing. Cell *133*, 585–600.

Zhang, Z., Pinto, A.M., Wan, L., Wang, W., Berg, M.G., Oliva, I., Singh, L.N., Dengler, C., Wei, Z., and Dreyfuss, G. (2013). Dysregulation of synaptogenesis genes antecedes motor neuron pathology in spinal muscular atrophy. Proc. Natl. Acad. Sci. USA *110*, 19348–19353.